

Mechanical property evaluation of an Al-2024 alloy subjected to HPT processing

Deepak C Patil¹, K Venkateswarlu², S A Kori³, Goutam Das⁴,
Mousumi Das⁴, Saleh N Alhajer⁵ and Terence G Langdon⁶

¹ KLE Dr. M. S. Sheshgiri College of Engineering and Technology, Udyambag, Belgaum-590008, India

² CSIR-National Aerospace Laboratories, Bangalore-560017, Karnataka, India

³ Basaveshwar Engineering College, Bagalkot-587102, Karnataka, India

⁴ CSIR-National Metallurgical Laboratory, Jamshedpur-831007, India

⁵ Department of Manufacturing Engineering, College of Technological Studies, PAAET, 70654 Shuwaikh, 5Kuwait.

⁶ Materials Research Group, Faculty of Engineering and the Environment, University of Southampton, Southampton, SO17 1BJ, UK

E-mail: todeepakpatil@rediffmail.com

Abstract. An aluminum-copper alloy (Al-2024) was successfully subjected to high-pressure torsion (HPT) up to five turns at room temperature under an applied pressure of 6.0 GPa. The Al-2024 alloy is used as a fuselage structural material in the aerospace sector. Mechanical properties of the HPT-processed Al-2024 alloy were evaluated using the automated ball indentation technique. This test is based on multiple cycles of loading and unloading where a spherical indenter is used. After two and five turns of HPT, the Al-2024 alloy exhibited a UTS value of ~1014 MPa and ~1160 MPa respectively, at the edge of the samples. The microhardness was measured from edges to centers for all HPT samples. These results clearly demonstrate that processing by HPT gives a very significant increase in tensile properties and the microhardness values increase symmetrically from the centers to the edges. Following HPT, TEM examination of the five-turn HPT sample revealed the formation of high-angle grain boundaries and a large dislocation density with a reduced average grain size of ~80 nm. These results also demonstrate that high-pressure torsion is a processing tool for developing nanostructures in the Al-2024 alloy with enhanced mechanical properties.

1. Introduction

Al-2024 is a high strength alloy at room temperature and even at elevated temperatures. In addition, it displays superior finish ability and fair to good workability together with good machinability. This alloy shows a relatively low ductility at room temperature and is generally heat treated in various conditions to suit particular applications. It finds wide use in many aerospace structural elements, military vehicles, bridges and weapons manufacture because of its excellent strength. Therefore, further improvements in the mechanical properties of this alloy will open up new areas of research.

Severe plastic deformation (SPD) technologies provide new opportunities for developing nanostructures in metals and alloys with improved mechanical properties that are very attractive for various structural and functional applications [1]. The fine refinement in the structure of metals and alloys developed by modern methods of SPD has led to the development of newer ultrafine-grained (UFG) materials with a unique set of functional and service properties [2]. Because of their microstructural instability, UFG pure metals are less applicable for engineering needs and hence alloying has been employed to stabilize ultrafine grains by reducing the grain-boundary energy [3, 4]. The strengthening effects, including grain refinement, dislocation entanglements, solid solutions and precipitation influence the



high strength in UFG alloys. Several SPD techniques are now available but most attention to date has centered on processing by equal-channel angular pressing (ECAP) [5], repetitive corrugation and straightening (RCS) or high-pressure torsion (HPT) [6-8].

In equal-channel angular pressing (ECAP), which is also known as equal-channel angular extrusion, a well-lubricated specimen is pressed through a die having a pair of intersecting channels of uniform cross-section. During ECAP, an extremely high shear strain is accumulated in the material due to the simple shear applied to the sample at the intersection of the channels [9]. The magnitude of this shear is determined by the channel angle Φ (angle of channel intersection) and the angle associated with the arc of curvature. Usually the channels will be square or circular in cross-section and samples or billets with the same cross-sections as the channels can be rotated by either 90° or any increment of 90° between each pass. According to this rotation around the longitudinal axis of the sample, different processing routes may be developed. It is observed that the processing route has a major influence on the effectiveness of ECAP processing with respect to grain refinement together with the fragmentation and modification of the precipitate distribution [10]. Processing by ECAP, which was developed by Segal and his associates three decades ago [11-13], is now recognized as a novel procedure for the fabrication of ultrafine-grained (UFG) metals and alloys.

Among the various SPD techniques, processing by HPT has proven to be most effective in producing bulk nanostructured materials possessing exceptionally small grain sizes. Among the various SPD techniques, HPT is especially attractive because it is easy to carry out, it has the ability to apply extremely high strains and it generally produces exceptionally small grain sizes. HPT applies a defined continuous variation of strain whereas most SPD processes offer only a stepwise application of strain. Furthermore, with HPT relatively brittle or high strength materials can be severely deformed and this is often not possible using other SPD processes. When HPT processing is applied to a thin circular disk, the disk is placed between two heavy anvils, subjected to an applied pressure, and then strained torsionally through rotation of one of the anvils. The applied pressure produces compressive stresses that are effective in preventing cracking of the sample, whereas the torsional straining developed by the anvil rotation produces severe plastic deformation of the thin disk. The samples processed by HPT are generally in the form of thin circular disks having diameters of 10-12 mm and 0.4-0.85 mm thickness.

Based on the anvil rotation, HPT can be either monotonic-HPT (m-HPT) or cyclic-HPT (c-HPT). In monotonic HPT, the anvil is rotated in a single direction and it is possible to periodically reverse the strain direction in HPT using the procedure, which is termed cyclic HPT. It has been reported that strain reversal by cyclic-HPT retards the formation of high-angle grain boundaries (those having misorientations larger than 20°) in pure aluminium [14].

The present paper reports on microstructural examinations and microhardness measurements carried out on a commercial Al-2024 alloy processed by HPT. The intent was to explore the effectiveness of the HPT process for grain refinement and subsequent enhancement of mechanical properties in the Al-2024 alloy.

2. Experimental material and procedures

The high-strength aluminum alloy considered in this investigation belongs to the Al-Cu alloy family. Such alloys are especially designed for their superior mechanical properties for use in

crucial structural parts of aircraft. Experiments were conducted on a commercial Al-2024 alloy containing, in wt%, 5.0 % Cu, 0.64 % Mg, 0.75 % Mn, 0.98 % Si, 0.37 % Fe, 0.01 % Cr, 0.09 % Zn, and 0.15 % others with the remaining as aluminium. It should be noted that this Al-2024 alloy is regularly used for various components in the aerospace industry as, for example, in the airframes of the fuselage. This unique aluminium alloy is well known to be very damage tolerant and exhibits good fatigue properties. It is also renowned for its good mechanical properties, its lightweight characteristics and its general overall resistance to corrosion.

The Al-2024 material was received in a T-5 condition in the form of a rod with a diameter of 12.5 mm and with a length of 80 mm. The rod was machined to a diameter of 10 mm and then disk samples were prepared for HPT processing. Each disk was sliced from the rod having parallel faces of 1.5 mm thickness using an electric discharge machining facility. These disks were then polished on both sides using 180 grit to 4000 grit abrasive papers sequentially in order to obtain a smooth surface and a uniform thickness of 0.83 mm.

The HPT disk of the Al-2024 alloy was then placed in a central circular shallow depression on the lower HPT anvil and the lower anvil was raised into contact with the upper anvil which had a similar shallow depression at its center. A load of 471 kN was applied on the anvils, leading to a pressure of 6.0 GPa on the contact surfaces of the sample. The details of HPT processing were described in earlier reports [15-18]. In the present experiments, HPT processing was carried out using a quasi-constrained HPT facility for $\frac{1}{4}$, $\frac{1}{2}$, $\frac{3}{4}$, 1, 2, and 5 numbers of anvil revolutions for separate samples. After the HPT processing, every disk was polished carefully on one side with the final polishing performed using a 0.02 μm alumina suspension.

An Automated Ball-Indentation (ABI) technique was employed to assess the mechanical properties of the HPT-processed specimens. It was necessary to use a non-destructive testing (NDT) technique for evaluating the mechanical properties of HPT-processed samples due to their small dimensions and the ABI technique served this purpose admirably. The ABI technique works on the principle based on the strain produced in several indentations at a single penetration position on a polished surface by a small spherical indenter [19, 20]. The indenter depth is gradually increased to a maximum limit which is specified by the user with intermediate partial unloading. In the present experiments, a WC ball with 1.57 mm diameter was indented on each test sample, both at the centre and also at a point near the edge, using an indentation speed of 0.5 mm min⁻¹. A load cell of 2500 N and loads up to 1000 N were used in these experiments. A velocity of 0.5 mm min⁻¹ was maintained during repetitive sequences of loading, unloading and reloading to set up multiple load-deflection curves. By the use of software, the machine automatically plots curves of true stress vs. true plastic strain from these load-deflection curves. Finally, the yield strength of the material, the ultimate tensile strength and the strain hardening coefficient for HPT-processed samples were obtained from the true stress vs. true plastic strain curves [21].

In practice, the microhardness varies symmetrically about the centre of the HPT-processed specimens due to the lower imposed strain in the central area of the disk leading to lower microhardness whereas higher microhardness was achieved at the peripheral area receiving a high imposed strain [22]. Values of the Vickers microhardness, Hv, were recorded along the diameters of all disks using a Leica VHMT auto-microhardness tester equipped with a Vickers diamond indenter. The microhardness was measured with an applied load of 25 g and a dwell time of 15 s along the diameter of each specimen, starting from one edge to the diametrically opposite edge and passing through the centre of the specimen using

incremental steps of 0.5 mm. The microhardness values were recorded for all of the HPT-processed samples and also for an as-received and unprocessed sample.

The microstructures of the HPT-processed samples were examined by transmission electron microscopy (TEM) using a Philips CM2000 TEM. TEM samples with a small diameter of 3 mm were punched from HPT-processed disks at a distance of approximately 2 mm from the disk center and these disks were further electro-polished in a twin-jet polishing facility using a perchloric acid-ethanol mixture maintained at 253 K. Microstructural observations of the as-cast specimens was carried out using optical microscopy and a scanning electron microscope (SEM). For the SEM, the specimens were mechanically polished to a mirror-like finish and deep etched with a water solution of HCl and HF to permit an analysis of the grain sizes and distributions within the Al matrix.

3. Results and discussion

3.1 Variation of microhardness after HPT

The Vickers microhardness across the surface of unprocessed Al-2024 alloy was $H_v \sim 138$ and Fig. 1 shows the variation of Vickers microhardness values recorded on the surfaces of the HPT-processed disks. In this figure, the Vickers, microhardness is plotted against the distance from the centre of the processed disks on either side of the center. It is apparent that these values continuously decrease from the edge towards the disk centres and then gradually increase from the disk centres towards the other edges for all HPT-processed disks. It can be seen from the figure that, as the number of HPT turns increases, the overall Vickers microhardness across the disk surface increases and also the microhardness in the outer region is always higher than in the centre for all HPT-processed disks. This result is predictable from the nature of the HPT process which imposes a higher strain in the peripheral area of the disk leading to higher values of microhardness whereas a lower microhardness is achieved in the central area because it is subjected to a smaller amount of strain.

After HPT processing, there is a considerable increase in the microhardness value at the centre of the disk after 5 turns whereas it is negligible up to $3/4$ turns. By contrast, there is a considerable increase in the microhardness at the peripheral area of the disk with a value of $H_v \sim 249$ after 5 turns. After processing by HPT, there is a nominal decrease in the initial disk thickness of ~ 0.83 mm. The measured thicknesses at the centres of the disks were ~ 0.824 mm after $1/4$ turn, ~ 0.818 mm after $1/2$ turn, ~ 0.808 mm after $3/4$ turn, ~ 0.799 mm after 1 turn, ~ 0.792 mm after 2 turns and ~ 0.785 mm after 5 turns.

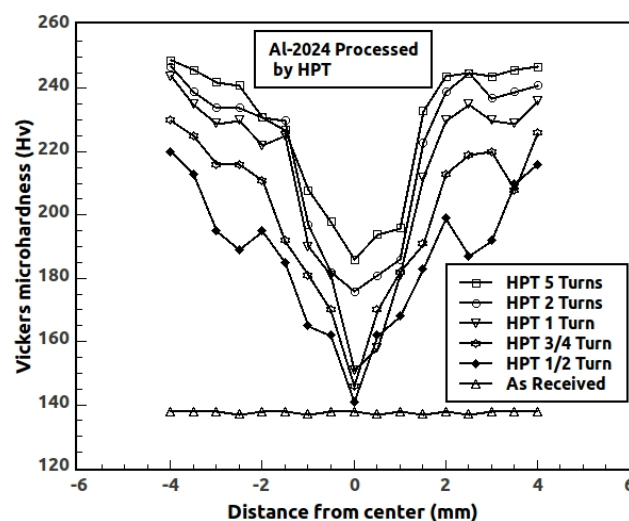


Fig. 1 The average Vickers microhardness, Hv, versus distance from the centres of the Al-2024 disks

3.2 Enhanced mechanical properties after HPT

The yield strength (YS), ultimate tensile strength (UTS), and the strain-hardening coefficient (n) are the various mechanical properties determined by using the ABI technique for the different specimens processed by HPT. Table 1 summarizes the ABI results at both the centre and edge for various samples.

Table 1 ABI results of the HPT-processed Al-2024 alloy

No. of Turns	Position	YS (MPa)	UTS (MPa)	n
1/4 turn	Centre	276	696	0.141
	Edge	319	823	0.118
1/2 turn	Centrr	282	706	0.134
	Edge	337	833	0.113
3/4 turn	Centre	291	731	0.129
	Edge	352	879	0.108
1 turn	Centre	311	762	0.121
	Edge	386	945	0.106
2 turns	Centre	325	791	0.116
	Edge	412	1014	0.105
5 turns	Centre	340	815	0.106
	Edge	510	1160	0.098

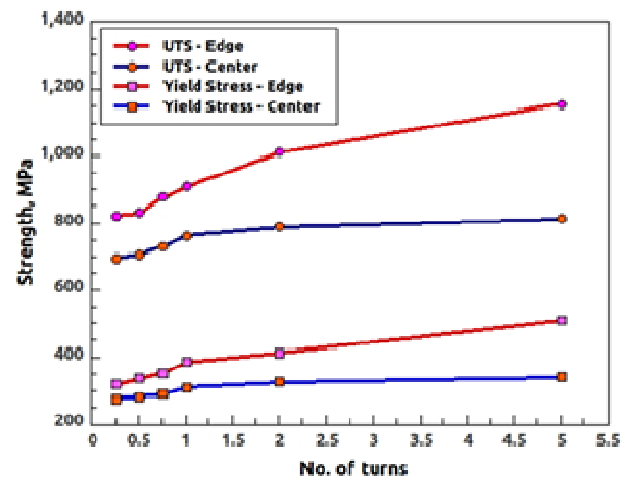


Fig. 2 UTS and YS variation at the edge and centre of disks processed by increasing numbers of HPT turns

Fig. 2 shows the variation of the yield strength and ultimate tensile strength at both the centre and edge of the HPT-processed specimens with increasing numbers of HPT turns. The lower pair of curves exhibit the improvement in yield strength whereas the upper pair of curves illustrate the continued enhancement of the ultimate tensile strength as the number of HPT turns increases. From Fig. 2 it can be seen that the values of the ultimate tensile strength and also the values of the yield strength at the edges of the processed specimens are consistently higher than those at the centres.

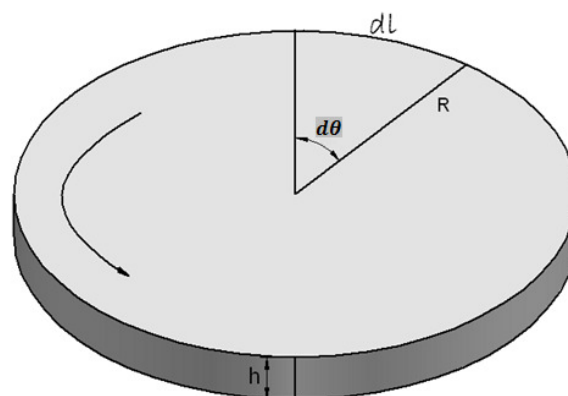


Fig. 3 Estimation of equivalent strain induced in HPT-processed disk

The principle for measuring the strain in HPT processing is illustrated schematically in Fig. 3 where a disk of radius R is subjected to a small torsional rotation $d\theta$. The consequent

displacement along the circumference of the disk will be $d\ell$ which equivalent is to $Rd\theta$. This induces an incremental shear strain $d\gamma = Rd\theta/h$, where h is the thickness of the disk. Hence, the equivalent von Mises strain imposed on the disk subjected to N number of HPT turns is given by

$$\epsilon = \frac{\gamma}{\sqrt{3}} = \frac{R\theta}{\sqrt{3}h} = \frac{2\pi NR}{\sqrt{3}h} \quad (1)$$

Equation (1) clearly suggests that the equivalent strain induced in the HPT disk is proportional to the distance from the centre of the disk. This is evident from the results of yield strength and ultimate tensile strength described in Table 1 which show higher values of strength at the circumference of disks and lower values at the centre for all of the disks processed by various numbers of HPT turns.

3.3 Microstructural observations

Characteristic microstructures of the Al-2024 alloy in the as-received condition without HPT processing are shown in Fig. 4 by means of optical microscopy and SEM. The average grain size of the as received and unprocessed Al-2024 specimens was $\sim 40 \mu\text{m}$ which is evident from the appearance in optical microscopy and from similar photomicrographs recorded using SEM.

The microstructural developments at the edge region of the Al-2024 alloy processed by 5 turns of HPT deformation is illustrated in Fig.5 (a) by the TEM micrograph. Fig. 5 (a) illustrates a homogeneous nanocrystalline distribution where many grain boundaries of the nanocrystalline grains are not well defined. The grain size throughout the sample appears uniform, thereby indicating a regular grain refinement from coarse grains to nano-structured grains. The HPT processing gave rise to substantial grain refinement and to a mean grain size

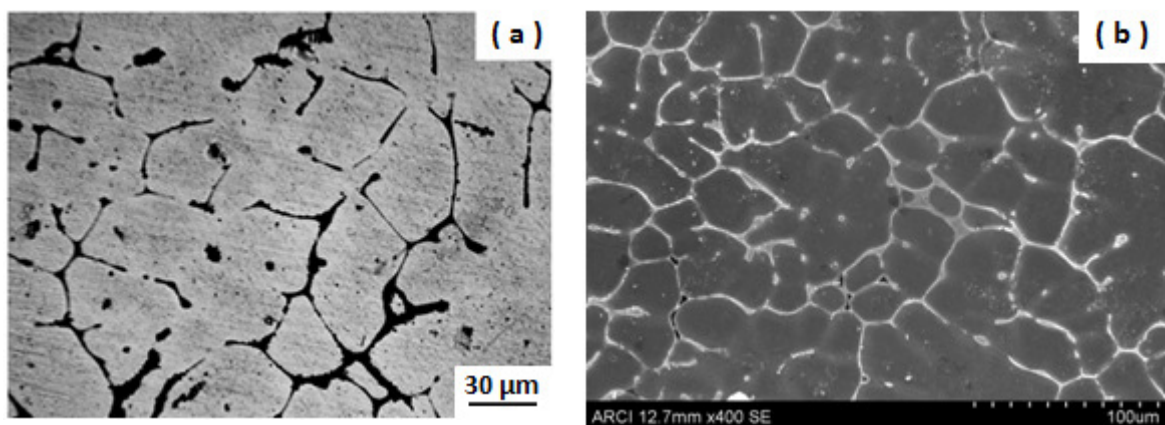


Fig. 4. Microstructure of Al-2024 alloy in the as-received condition by means of (a) optical microscopy and (b) SEM

of ~80 nm. HPT processing achieves maximum grain refinement because of the high amount of straining achieved by the combined effect of compression and subsequent torsion. Compared to other types of SPD techniques like RCS and ECAP, HPT introduces a very high density of dislocations into the specimens. The TEM microstructure shown in Fig. 5 (a), and the supporting selected area diffraction pattern in Fig. 5(b), reveal dislocation cells and dislocation-tangles in the heavily deformed grains of the alloy. Even though the grain boundaries are mostly poorly defined, some grain boundaries are identifiable and a portion of these are still curved or wavy which indicates they are in a non-equilibrium state.

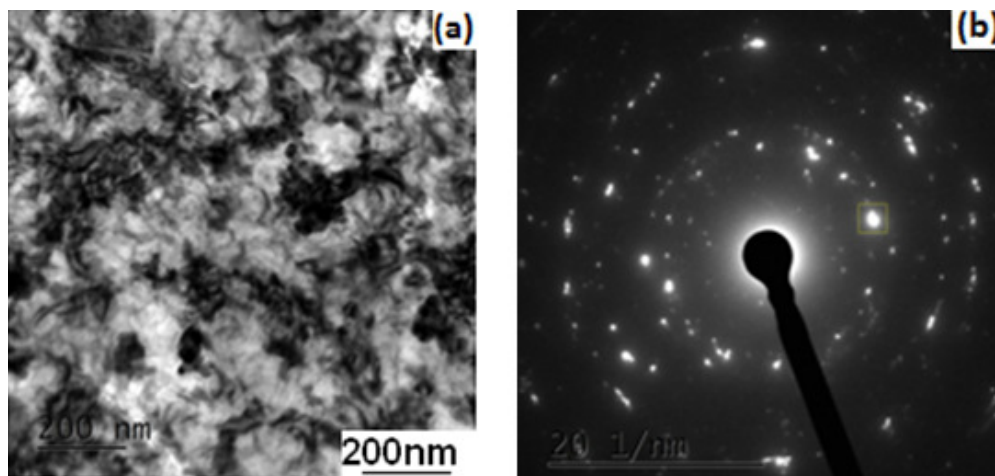


Fig. 5. (a) A TEM image taken near the edge of 5 turn HPT sample (b) selected area diffraction pattern for the same

4. Summary and conclusions

1. HPT processing was successfully conducted on a commercial Al-2024 alloy for up to a maximum of 5 turns. The processing was carried out under an applied pressure of 6.0 GPa and at room temperature.
2. Through use of the ABI technique, it is shown that both the yield strength and the ultimate tensile strength of HPT-processed Al-2024 alloy increase with increasing numbers of HPT turns. However, the rate of increase in the ultimate tensile strength is found to be higher than that of the yield strength.
3. The value of the strain hardening coefficient decreases with the increasing number of HPT turns, indicating that the formability of the Al-2024 alloy decreases with increasing numbers of HPT turns.
4. Detailed microhardness measurements show that HPT is very efficient in producing high hardness near the circumference of the processed samples and the heterogeneity of hardness values from the circumference to the center of the processed samples can be minimized by processing with higher numbers of HPT turns.
5. TEM images suggest the formation of nanostructures in Al-2024 alloy after processing by 5 turns of HPT with a grain size of ~80 nm which enhanced the ultimate tensile strength to ~1160 MPa at the edge of the disk after 5 turns.

References

- [1] Liu M, Roven H J, Liu X, Murashkin M, Valiev R Z, Ungar T, Balogh L 2010 *Trans of Nonferrous Met Soc of China* **20** 2051
- [2] Brodova I G, Shirinkina I G, Petrova A N, Antonova O V, Pilyugin V P 2011 *The Physics of Metals and Metallography* **111** 630
- [3] Kirchheim R 2007 *Acta Mater* **55** 5125
- [4] Choi P, Da Silva M, Klement U, Al-Kassab T, Kirchheim R 2005 *Acta Mater* **53** 4473
- [5] Venkateswarlu K, Rajinikanth V, Ray A K, Xu C, Langdon T G 2010 *Mater Sci Eng A* **527** 1448
- [6] Rajinikanth V, Venkateswarlu K, Mani Kuntal S, Mousami D, Alhajeri S N, Langdon T G 2011 *Mater Sci Eng A* **528** 1702
- [7] Langdon T G 2013 *Acta Mater* **61** 7035
- [8] Venkateswarlu K, Rajinikanth V, Mani Kuntal S, Alhajeri S N, Langdon T G 2011 *Mater Sci Forum* **667** 743
- [9] Djavanroodi F, Ebrahimi M 2010 *Mater Sci Eng A* **527** 1230
- [10] Liang W, Bian L, Xie G, Zhang W, Wang H, Wang S 2012 *Mater Sci Eng A* **527** 5557
- [11] Segal V M 1977 USSR Patent No. 575892
- [12] Segal V M, Reznikov V I, Drobyshevskiy A E, Kopylov V I 1981 *Russian Metallurgy* **1** 99
- [13] Kim H S 2001 *Mater Sci Eng A* **315** 122
- [14] Orlov D, Todaka Y, Umemoto M, Tsuji N 2009 *Mater Sci and Eng A* **499** 427
- [15] Patil D C, Kori S A, Venkateswarlu K, Goutam D, Alhajeri S N, Langdon T G 2013 *Journal of Mater Sci* **48** 4773
- [16] Kawasaki M, Langdon T G 2008 *Mater Sci Eng A* **498** 341
- [17] Kawasaki M, Figueiredo R B, Langdon T G 2011 *Acta Mater* **59** 308
- [18] Kawasaki M 2014 *J Mater Sci* **49** 18
- [19] Goutam D, Ghosh S, Ghosh R N 2005 *Mater Sci Eng A* **408** 158
- [20] Goutam D, Mousume D, Subhasis S, Chakraborty S 2009 *Mater Sci Eng A* **513** 389
- [21] Venkateswarlu K, Goutam D, Pramanik A K, Xu C, Langdon T G 2006 *Mater Sci Eng A* **427** 188
- [22] Jiang H, Zhu Y T, Butt D P, Alexandrov IV, Lowe T C 2000 *Mater Sci Eng A* **290** 128